Perivascular stem cells

aDental and Craniofacial Research Institute, bSection of Orthodontics, School of Dentistry, and gDepartment of Bioengineering, University of California, Los Angeles, Los Angeles, California, USA; cDepartment of Orthopaedic Surgery and dOrthopaedic Hospital Research Center, Orthopaedic Hospital/University of California, Los Angeles, Los Angeles, California, USA; ePrivate practice, Marina del Rey, California, USA; fDivision of Plastic and Reconstructive Surgery, University of Southern California, Los Angeles, California, USA; hCenter for Cardiovascular Science and MRC Center for Regenerative Medicine, University of Edinburgh, Edinburgh, United Kingdom

*Contributed equally as first authors.

Correspondence: Chia Soo, M.D., Department of Orthopaedic Surgery, University of California, Los Angeles, 675 Charles E. Young Drive South, MRL 2641A, Los Angeles, California 90095-1579, USA. Telephone: 310-794-5479; Fax: 310-206-7783; e-mail: bsoo@ucla.edu; or Kang Ting, D.M.D., D.Med.Sc., Section of Orthodontics, UCLA School of Dentistry, CHS 30-117, 10833 Le Conte Avenue, Los Angeles, California 90095, USA. Telephone: 310-206-6305; Fax: 310-206-5349; kting@dentistry.ucla.edu; or Bruno Péault, Ph.D., Department of Orthopaedic Surgery, David Geffen School of Medicine at UCLA, Orthopaedic Hospital Research Center, Box 957358, Los Angeles, California 90095-7358. Telephone: 310-794-1339; Fax: 310-825-5409; e-mail: bpeault@mednet.ucla.edu

Perivascular Stem Cells: A Prospectively Purified Mesenchymal Stem Cell Population for Bone Tissue Engineering

AARON W. JAMES,a,b,c,d* JANETTE N. ZARA,c,d* XINLI ZHANG,a,b ASAL ASKARINAM,a,b RAGHAV GOYAL,a,b MICHAEL CHIANG,a,b WEI YUAN,c,d LE CHANG,a,b MIRKO CORSELLI,c,d JIA SHEN,a,b SHEN PANG,a,b DAVID STOKER,e,f BEN WU,g KANG TING,a,b,c,d BRUNO PÉAULT,c,d,h CHIA SOOc,d

ABSTRACT

Adipose tissue is an ideal source of mesenchymal stem cells for bone tissue engineering: it is largely dispensable and readily accessible with minimal morbidity. However, the stromal vascular fraction (SVF) of adipose tissue is a heterogeneous cell population, which leads to unreliable bone formation. In the present study, we prospectively purified human perivascular stem cells (PSCs) from adipose tissue and compared their bone-forming capacity with that of traditionally derived SVF. PSCs are a population (sorted by fluorescence-activated cell sorting) of pericytes (CD146+CD34−CD45−) and adventitial cells (CD146−CD34+CD45−), each of which we have previously reported to have properties of mesenchymal stem cells. Here, we found that PSCs underwent osteogenic differentiation in vitro and formed bone after intramuscular implantation without the need for predifferentiation. We next sought to optimize PSCs for in vivo bone formation, adopting a demineralized bone matrix for osteoinduction and tricalcium phosphate particle formulation for protein release. Patient-matched, purified PSCs formed significantly more bone in comparison with traditionally derived SVF by all parameters. Recombinant bone morphogenetic protein 2 increased in vivo bone formation but with a massive adipogenic response. In contrast, recombinant Nel-like molecule 1 (NELL-1; a novel osteoinductive growth factor) selectively enhanced bone formation. These studies suggest that adipose-derived human PSCs are a new cell source for future efforts in skeletal regenerative medicine. Moreover, PSCs are a stem cell-based therapeutic that is readily approvable by the U.S. Food and Drug Administration, with potentially increased safety, purity, identity, potency, and efficacy. Finally, NELL-1 is a candidate growth factor able to induce human PSC osteogenesis. STEM CELLS TRANSLATIONAL MEDICINE 2012;1:510–519

INTRODUCTION

Since the original description of adipose tissue as a source of adult multilineage stem cells [1], the preclinical study of adipose-derived cells for repair and regeneration of tissues has increased dramatically (reviewed in [2]). The theoretical advantages of adipose-derived cells over other cell types for biologic bone regeneration strategies are numerous. For example, although autograft bone remains the gold standard for bone repair, its disadvantages are significant, including donor site morbidity, extended operating time complications, and limited autogenous supply [3–5]. On the other hand, bone marrow mesenchymal stem cells (BMSCs) have long been studied for their application to skeletal engineering. However, BMSCs have distinct disadvantages over adipose-derived cells, including limitations in autogenous supply of bone marrow aspirate as compared with lipoaspirate, and relatively lower

cell yield of BMSCs in comparison with adipose-derived stem cells (ASCs) (estimated at $\sim 10^4$ stem cells vs. $\sim 10^6$ stem cells per 40 ml) [6–8]. Finally, human ASCs have been used successfully to heal small animal [9, 10] and large animal [11] skeletal defects.

Despite the advantages of fat tissue-derived cells for bone regeneration, there exist clear hurdles that must be overcome for their successful clinical use. For example, adipose-derived stromal cells are defined by their adherence to cell culture plates and ex vivo expansion. This ex vivo expansion increases the risk of immunogenicity, infection, and genetic instability [12, 13]. As an alternative to ASCs, the cells of noncultured total stromal vascular fraction (SVF) from adipose tissues have been used. Available studies using SVF show poor and unreliable bone formation [14] or lower bone regeneration efficacy relative to cultured ASCs [15]. SVF of adipose tissue is a highly

heterogeneous cell population, including nonmesenchymal stem cell types, such as inflammatory cells, hematopoietic stem cells, and endothelial cells, among others [16]. Variability in cell composition presents clear disadvantages for U.S. Food and Drug Administration (FDA) approval of a future stem cell-based therapeutic, potentially including reduced safety, purity, identity, potency, and efficacy. Notably, these are the criteria upon which the Center for Biologics Evaluation and Research evaluates stem cell-based product applications [17]. For example, given the heterogeneity of SVF, precise product characterization is not feasible, leading to lack of human stromal vascular fraction (hSVF) product identity. Batch-to-batch variability and nonuniformity in effect (again attributable to variable stem cell content) reduces the efficacy and potency of hSVF compounds and potentially reduces product safety. With these regulatory hurdles in mind, our approach was to reduce the inherent heterogeneity within hSVF to obtain a safer and more efficacious stem cell-based therapeutic.

To address this issue of SVF heterogeneity, previous investigators have used fluorescence-activated cell sorting (FACS) to purify fat-derived cell populations, with some success. For example, cell sorting of adipose tissue has allowed for enrichment of osteoprogenitor [18] or chondroprogenitor [19] cell types—but not the isolation of multipotent mesenchymal stem cells (MSCs). Our solution has been to identify the native perivascular phenotype of MSCs and prospectively isolate perivascular MSCs using multicolor FACS. We have previously shown two populations of perivascular stem cells (PSCs) associated with blood vessels [20–24]. These include CD34−CD146+CD45− pericytes surrounding microvessels and capillaries [20, 25] and a second distinct adventitial cell (CD34+CD146−CD45−) [26], associated with larger blood vessels. Both cell types are isolatable from adipose tissue and resemble MSCs by morphology, growth, surface markers, and clonal multilineage differentiation potential [20–24].

In this report, we describe the use of a novel, FACS-purified cell source for improved bone tissue engineering: human perivascular stem cells (hPSCs). Using an intramuscular, ectopic bone model, we observed that adipose-derived, FACS-isolated hPSCs formed bone to a greater degree than patient-matched, unsorted hSVF. Next, two growth factors were examined for their osteoinductive effects: bone morphogenetic protein 2 (BMP2) and Nel-like molecule-1 (NELL-1). The novel cytokine NELL-1 was identified as an appropriate osteogenic stimulus rather than BMP2, which had pleiotropic effects, including adipogenic differentiation and cyst-like bone formation.

MATERIALS AND METHODS

Isolation of SVF from Human Lipoaspirate

Human lipoaspirate ($n = 70$ donors) was obtained from patients undergoing cosmetic liposuction. No patient identifiers were obtained. Lipoaspirate was stored for no more than 128 hours at 4°C before processing. The hSVF was obtained by collagenase digestion as previously described [26]. Briefly, lipoaspirate was diluted with an equal volume of phosphate-buffered saline (PBS) before digestion with Dulbecco's modified Eagle's medium (DMEM) containing 3.5% bovine serum albumin (Sigma-Aldrich, St. Louis, http://www.sigmaaldrich.com) and 1 mg/ml type II collagenase for 70 minutes under agitation at 37°C. Next, adi-

pocytes were separated and removed by centrifugation. The pellet was then resuspended in red-cell lysis buffer (155 mM NH_4Cl, 10 mM $KHCO_3$, and 0.1 mM EDTA) and incubated for 10 minutes at room temperature. After centrifugation, pellets were resuspended in PBS and filtered at 70 μm. The resulting hSVF was either further processed for cell sorting (to isolate PSCs) or used immediately for in vivo application. In order to calculate live cell number for implantation, trypan blue staining was performed to assess cell viability. Cells were kept on ice until in vivo implantation. $n = 70$ patient samples were used for in vitro experiments, and $n = 6$ patient samples were used for in vivo experiments; demographics were recorded, including age, sex, and anatomic location of harvest, and are presented in supplemental online Table 1.

Purification of PSCs from Human Lipoaspirate

PSCs were purified by FACS of the hSVF as previously described [26]. hSVF was incubated with a mixture of the following directly conjugated antibodies: anti-CD34-phycoerythrin (1:100; Dako, Glostrup, Denmark, http://www.dako.com), anti-CD45-allophycocyanin (1:100; Santa Cruz Biotechnology Inc., Santa Cruz, CA, http://www.scbt.com), and anti-CD146-fluorescein isothiocyanate (1:100; AbD Serotec, Raleigh, NC, http://www.ab-direct.com). All incubations were performed at 4°C for 15 minutes in the dark. Before sorting, 4′,6-diamidino-2-phenylindole (DAPI; 1:1,000; Invitrogen, Carlsbad, CA, http://www.invitrogen.com) was added for dead cell exclusion; the solution was then passed through a 70-μm cell filter and then run on a FACSAria cell sorter (BD Biosciences, San Diego, CA, http://www.bdbiosciences.com). Sorted cells were used for in vivo application immediately or plated for in vitro studies. In this manner, distinct microvessel pericytes (CD34−, CD146+, CD45−) and adventitial cells (CD34+, CD146−, CD45−) were isolated and combined to constitute the PSC population. For select experiments, fluorescent labeling of live cells was performed prior to implantation using PKH26 fluorescent cell linker (Sigma-Aldrich). Cells were kept on ice until in vivo implantation.

In Vitro Assays

The expansion of cells was performed in DMEM, 20% fetal bovine serum (FBS), 1% penicillin/streptomycin. Osteogenic differentiation of human PSCs was performed as previously described [9, 27], with minor modifications. Passage 4 PSCs were seeded at a density of 35,000 cells per well in 12-well plates. Differentiation medium consisted of DMEM, 10% FBS, 100 μg/ml ascorbic acid, and 10 mM β-glycerophosphate. Assessments, including alkaline phosphatase and alizarin red staining, were performed as previously described [10, 28].

Implant Preparation

Implants were prepared as per supplemental online Tables 2–5. Two different scaffolds were used for cell delivery. First, an absorbable collagen sponge of defined dimensions (0.5 × 1 × 1.5 cm) (component of the INFUSE Bone Graft; Medtronic, Minneapolis, MN, http://www.medtronic.com) was used (data presented in Fig. 1). This carrier was chosen as a nonosteoinductive carrier, as intramuscular implantation of absorbable collagen sponge alone is known to have no bone forming effects [29]. Second, an ovine DBX Putty was used (100 μl; Musculoskeletal Transplant Foundation, Edison, NJ, http://www.mtf.org). DBX Putty combines morselized cortical-cancellous demineralized
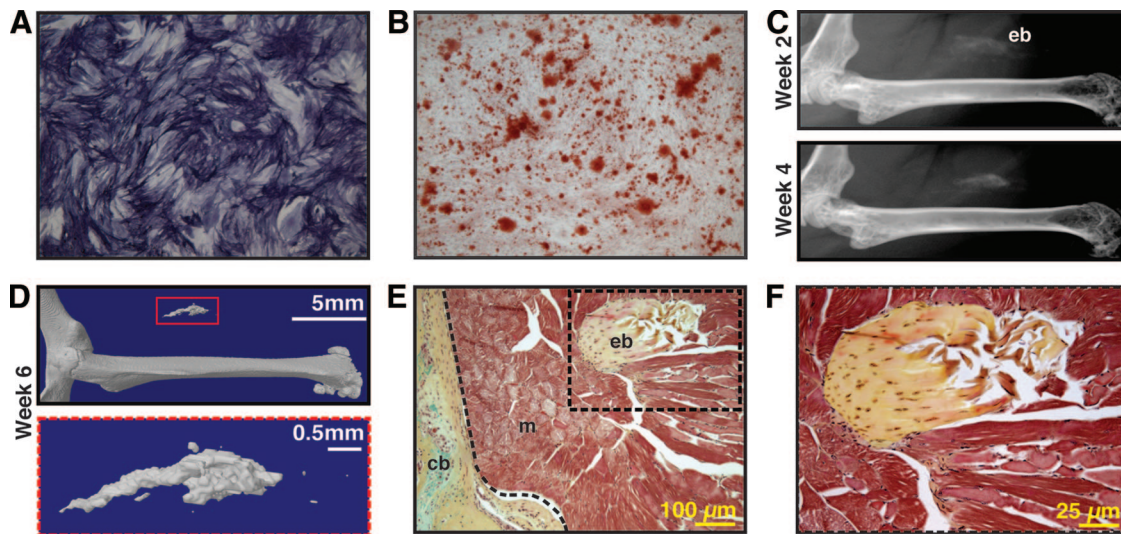
Figure 1. Human perivascular stem cells (hPSCs) are an osteocompetent cell population. **(A, B):** hPSCs were cultured under osteogenic conditions (10% fetal bovine serum, 100 μg/ml ascorbic acid, 10 mM β-glycerophosphate). **(A):** Representative image of alkaline phosphatase staining at 5 days of differentiation. **(B):** Representative image of alizarin red staining, 10 days of differentiation. **(C–F):** hPSCs were implanted in the thigh complex of a SCID mouse using a collagen sponge carrier (2.5×10^5 cells, sponge size $2.0 \times 1.0 \times 0.5$ cm). **(C):** High-resolution radiography at 2 and 4 weeks postimplantation. **(D):** Three-dimensional microcomputed tomography reconstructions at threshold 90. **(E, F):** Pentachrome staining of histological sections. $n = 5$ implants, from $n = 1$ patient specimens. See supplemental online Table 2 for treatment groups. Abbreviations: cb, cortical bone; eb, ectopic bone; m, muscle.

bone chips with sodium hyaluronate, and it was chosen for its proven osteoinductive characteristics and clinical translation (human demineralized bone matrix [DBX] is already 510(k) approved) (data presented in Figs. 2–5). Select experiments added growth factors (recombinant human BMP2 or NELL-1), which were lyophilized onto tricalcium phosphate (β-TCP) particles (Chronos β-TCP granules, 200–300 μm diameter; Synthes, West Chester, PA, http://www.synthes.com) and stored at 4°C prior to use. This avoids burst-type release kinetics in favor of sustained growth factor release [30]. Concentrations of BMP2 were based on the clinical-range doses needed for human bone formation (up to 1,500 μg/ml) rather than the lower doses more commonly used in mice [31]. Concentrations of NELL-1 were based on our previous publication using an intramuscular model and fetal pancreatic pericytes [32]. The individual components (DBX + β-TCP) were mixed mechanically prior to implantation. Finally, defined numbers of viable cells in PBS suspension (20 μl) from the hSVF or PSCs were applied (either allowed to soak into absorbable collagen sponge or mechanically mixed with DBX/β-TCP). The cell + scaffold suspension was kept on ice until implantation.

Surgical Procedures

Intramuscular implantation was performed in 8-week-old male SCID mice. Animals were anesthetized by isoflurane inhalation (5% induction, 2% maintenance) and premedicated with 0.05 mg/kg buprenorphine. Bilateral incisions in the hind limbs were made, and pockets were cut in the biceps femoris muscles by blunt dissection, parallel to the muscle fiber long axis. Implants were placed bilaterally; implant compositions are fully described in supplemental online Tables 2–6. Numbers of animals per experiment can be found in the figure legends. The fasciae overlying the muscle were sutured with a simple continuous pattern, and the skin was closed in a separate layer using 5-0 Vicryl (Ethicon, San Angelo, TX, http://www.ecatalog.ethicon.com) sutures in a subcuticular pattern. Animals were postoperatively treated

with buprenorphine for 48 hours and trimethoprim/sulfamethoxazole for 10 days for pain management and infection prevention, respectively. Animals were housed and experiments were performed in accordance with guidelines of the Chancellor's Animal Research Committee of the Office for Protection of Research Subjects at the University of California, Los Angeles.

Radiographic Imaging: High-Resolution XR and Quantitative Microcomputed Tomography Analysis

Live high-resolution radiographs were taken every 2 weeks for select experiments using a cabinet radiography system (Faxitron Bioptics, Lincolnshire, IL, http://www.faxitron.com). Mice were anesthetized using isoflurane (5% induction, 2% maintenance).

Samples were harvested en bloc from 4 to 6 weeks postimplantation, formalin-fixed, and imaged using high-resolution microcomputed tomography (microCT) (Skyscan 1172F; Skyscan, Kontich, Belgium, http://www.skyscan.be) at an image resolution of 19.73 μm and analyzed using DataViewer, Recon, CTAn, and CTVol programs provided by the manufacturer. For computed tomography (CT) data analysis, the region of interest includes the entire volume of the scanned muscle pouch excluding the native femur to quantify bone volume (BV) and bone mineral density (BMD). Threshold values for three-dimensional reconstructions and quantification can be found in the figure legends. All quantitative and structural morphometric data use nomenclature described by the American Society for Bone and Mineral Research Nomenclature Committee [33].

Histology and Immunohistochemistry Analysis

After CT analysis, samples were decalcified in 19% EDTA and embedded in paraffin. Hematoxylin and eosin (H&E) and Movat's pentachrome staining were performed as previously described [32]. For select experiments, bone formation was quantified by blinded histomorphometric analyses using H&E staining (Figs. 2, 6) and Photoshop (Adobe Systems Inc., San Jose, CA, http://
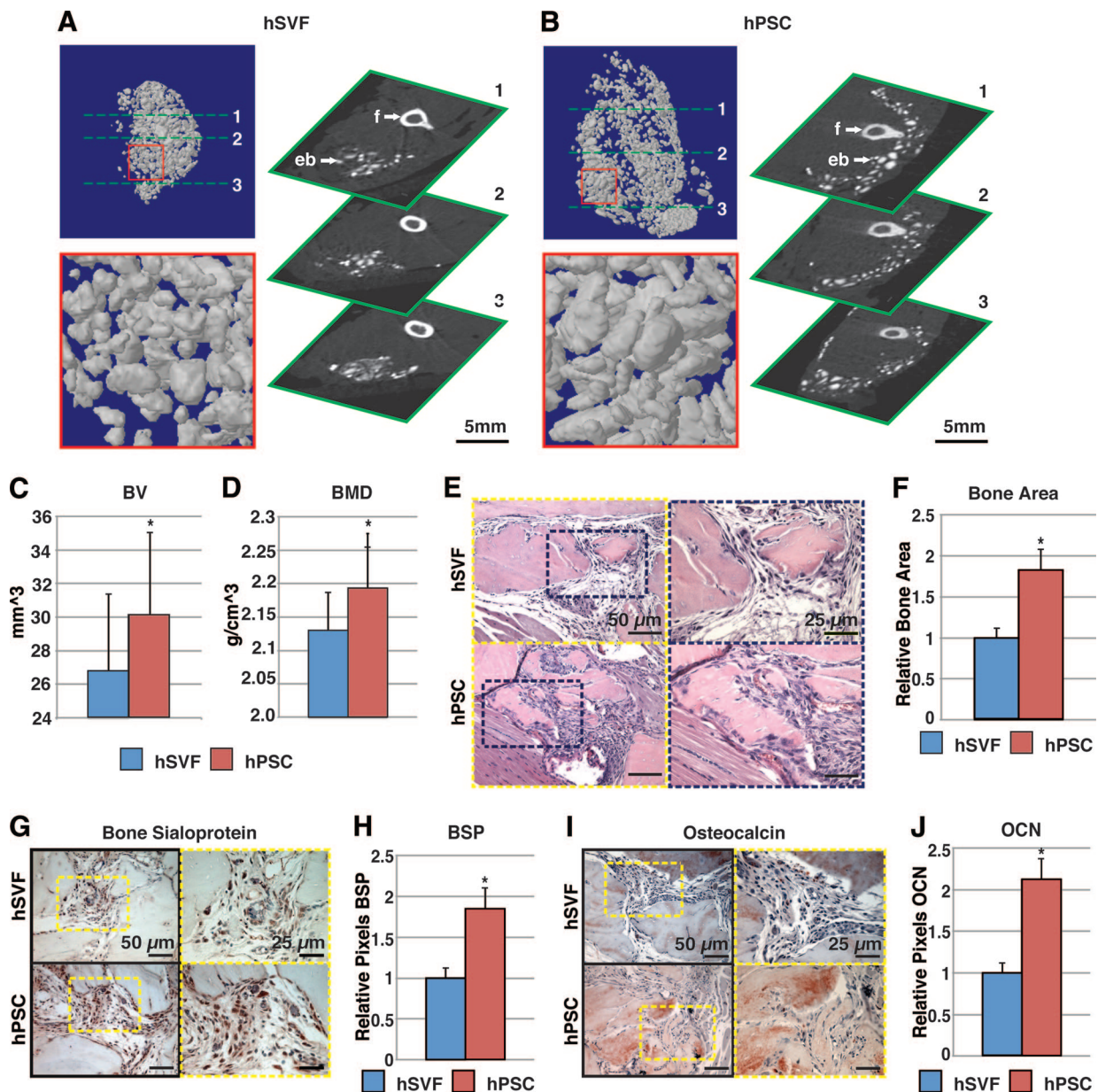
Figure 2. hPSCs undergo more robust differentiation in comparison with hSVF. Equal numbers of viable hSVF cells or hPSCs (2.5×10^5) from the same patient samples were implanted intramuscularly in the thigh of a SCID mouse. An osteoinductive DBX Putty was used as scaffold. Assessments were performed at 4 weeks postimplantation. **(A, B):** Microcomputed tomography (microCT) images of hSVF- and hPSC-treated samples. Representative three-dimensional microCT reconstructions at threshold (Th) 90 (left) and corresponding two-dimensional axial slices (right). **(C, D):** Analysis of BV and BMD among hSVF- and hPSC-treated samples; Th50–120. **(E):** Representative hematoxylin and eosin staining. **(F):** Representative histomorphometric quantification of bone area per ×100 field. **(G):** Representative BSP immunohistochemistry. **(H):** Quantification of relative staining per ×400 field. **(I):** Representative OCN immunohistochemistry. **(J):** Quantification of relative staining per ×400 field. Histomorphometric quantification calculated from $n = 6$ random microscopical fields. $n = 12$ implants per cell type, $n = 3$ patient specimens. See supplemental online Table 3 for treatment groups. ∗, $p < .05$ in comparison with control as assessed by Student's t test. Abbreviations: BMD, bone mineral density; BSP, bone sialoprotein; BV, bone volume; eb, ectopic bone; f, femur; hPSC, human perivascular stem cell; hSVF, human stromal vascular fraction; OCN, osteocalcin.

www.adobe.com) quantification as expressed by mean bone area and bone area/tissue area [34]. For select experiments, adipogenesis was quantified by blinded calculations of lipid droplet number per ×100 field (Fig. 4). Immunohistochemistry was performed with primary antibodies against bone sialoprotein (Chemicon, Temecula, CA, http://www.chemicon.com), osteocalcin (Santa Cruz Biotechnology), and major histocompatibility complex (MHC) class I surface antigen (Santa Cruz Biotechnol-

ogy) using the ABC (Vector Laboratories, Burlingame, CA, http://www.vectorlabs.com) method. Select quantification of immunohistochemistry was performed again using the magic wand tool in Photoshop with a tolerance setting of 30 (Fig. 2).

Statistical Analysis

Statistical analysis was performed using an appropriate analysis of variance test when more than two groups were compared,
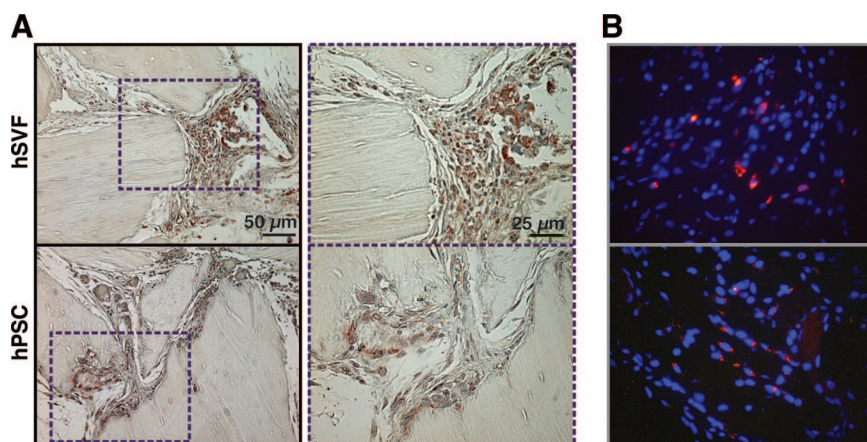
Figure 3. Persistence of hSVF or hPSCs after implantation. Shown are hSVF- or hPSC-treated samples implanted intramuscularly on a DBX Putty scaffold and assessed for cell persistence 4 weeks postimplantation. **(A):** Human major histocompatibility complex class I immunohistochemistry, indicating the presence of human xenografted cells. **(B):** Fluorescent cell labeling (PKH) performed prior to implantation. Red indicates persistence of human cells, and Hoechst nuclear counterstain appears blue. Abbreviations: hPSC, human perivascular stem cell; hSVF, human stromal vascular fraction.

followed by Student's *t* test to compare two groups. Inequality of SDs was excluded by using Levene's test. $p \leq .05$ was considered to be significant.

RESULTS

Stromal Vascular Fraction of Human White Adipose Tissue Contains Two Distinct Perivascular MSC Populations: Pericytes and Adventitial Cells

We recently described, purified, and characterized two perivascular sources of primary MSCs within human adipose tissue based on the expression of CD34 and CD146. Pericytes, which are surrounding microvessels, are isolatable from multiple human organs, including adipose tissue, and are CD146+CD34−CD45− [20, 25]. More recently, we have described a second and distinct perivascular MSC population, adventitial cells (CD146−CD34+CD45−) [26], obtainable from human adipose among other tissues. Here, we first confirmed our previous results, showing that pericytes (CD146+CD34−) and adventitial cells (CD146−CD34+) are distinct populations isolatable from human lipoaspirate after exclusion of CD45+ cells (hematopoietic cells) and DAPI+ cells (dead cells) (Fig. 6). Both pericytes and adventitial cells have been previously reported to undergo multiple mesodermal lineage differentiation [20, 26]. With $n = 70$ unique samples of lipoaspirate, we observed the mean prevalence of pericytes and adventitial cells to be 17.1% and 22.5% of the total viable cell yield of SVF. From a tissue-engineering standpoint, maximal MSC yield per unit of autologous tissue removed would improve efficacy for tissue engineering while reducing harvest morbidity. For this reason, we chose to combine both perivascular MSC populations—collectively termed PSCs—to maximize cell yield for our efforts in bone engineering (collectively, PSCs make up, on average, 39.6% of total viable SVF). Importantly, those cells within adipose tissue that are neither pericytes (CD146+CD34−) nor adventitial cells (CD146−CD34+) do not express typical MSC markers or undergo mesodermal lineage differentiation [26].

Perivascular Stem Cells Undergo Osteogenic Differentiation In Vitro and Form Bone In Vivo

hPSCs were first evaluated for their ability to undergo osteogenic differentiation in vitro and bone forming potential in vivo (Fig. 1). In standard osteogenic medium, hPSCs showed robust alkaline phosphatase staining after 5 days in differentiation medium and

bone nodule formation after 10 days in differentiation medium (Fig. 1A, 1B). Freshly derived hPSCs were next placed on a collagen sponge without predifferentiation or growth factor stimulation and inserted intramuscularly (see supplemental online Table 2 for treatment groups). Over the course of 6 weeks, spontaneous mineralization was observed by radiography (Fig. 1C), three-dimensional CT (Fig. 1D), and histology (Fig. 1E, 1F). In contrast, intramuscular implantation of absorbable collagen sponge alone is known to have no bone forming effects [29]. Collectively, these studies showed that hPSCs (like their individual pericyte and adventitial components) undergo osteogenic differentiation in vitro and in vivo and thus may be useful as a purified cell source for bone formation.
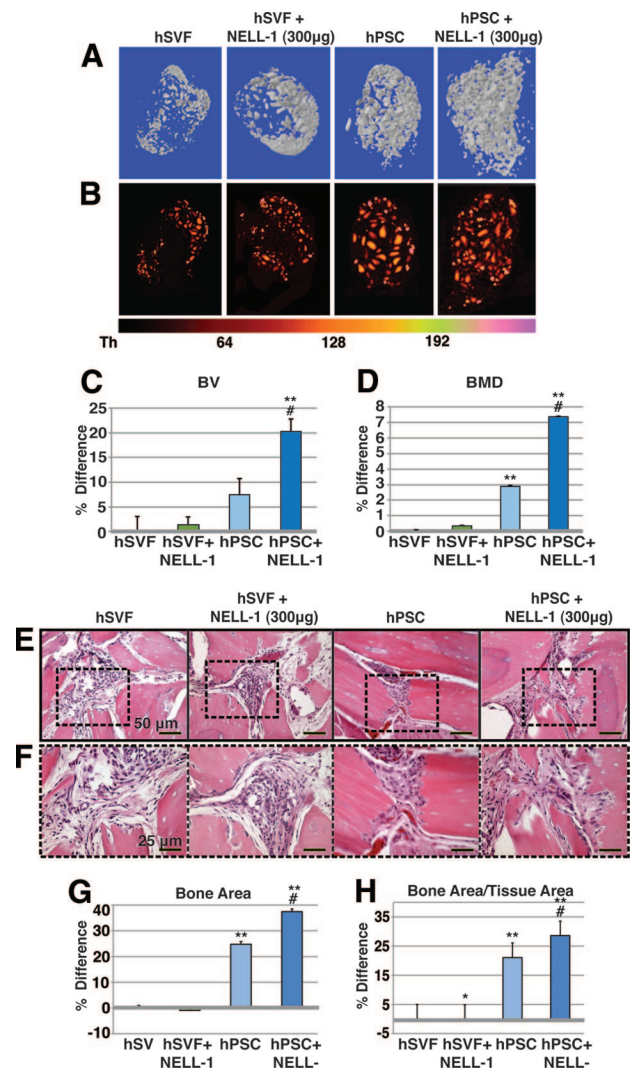
Human PSCs Undergo More Robust Bone Formation than hSVF Cells

Having demonstrated that hPSCs are an osteocompetent cell source, we next sought to directly compare bone formation in patient-matched, purified hPSCs to unsorted hSVF. For this head-to-head determination, the same numbers of viable hSVF cells or hPSCs were implanted (2.5×10^5) intramuscularly. An osteoinductive carrier was used: demineralized bone matrix (DBX Putty), which consists of morselized cortical-cancellous demineralized bone chips with sodium hyaluronate (Musculoskeletal Transplant Foundation) (see supplemental online Table 3 for treatment groups). At 4 weeks postimplantation, two- and three-dimensional CT images showed significantly increased bone formation in hPSC in comparison to hSVF samples (Fig. 2A, 2B). CT quantification demonstrated a statistically significant increase in BV and BMD in hPSC-treated samples (Fig. 2C, 2D). Histologic analysis was performed by routine H&E (Fig. 2E). Histomorphometric quantification of bone area per random high-powered field showed increased bone among hPSC-treated samples (Fig. 2F). Immunohistochemical staining for the bone-specific markers bone sialoprotein and osteocalcin was performed (Fig. 2G, 2I). In each instance, photographic quantitation of positive staining intensity showed a significant increase in both bone markers in hPSC-treated specimens (Fig. 2H, 2J). Importantly, we confirmed that those cells surrounding and interspersed between bone chips were of predominantly human origin (Fig. 3), using immunohistochemical staining for MHC class I human surface antigen (Fig. 3A) or via fluorescent labeling of hSVF cells or hPSCs prior to implantation (Fig. 3B). Thus, equivalent numbers of purified hPSCs result in increased ectopic bone formation in comparison with patient-matched hSVF cells.
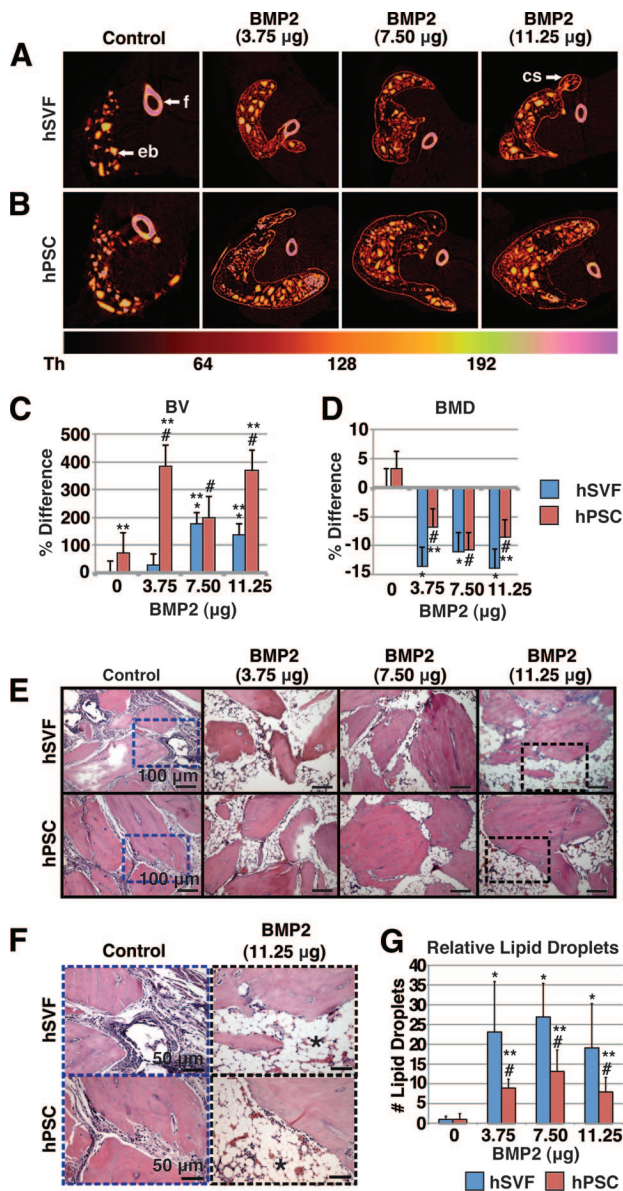
Figure 4. Effects of BMP2 on hSVF- or hPSC-mediated ectopic bone formation. hSVF or hPSCs were implanted intramuscularly with or without BMP2 on a DBX Putty (DBX) scaffold and assessed 4 weeks postimplantation. See supplemental online Table 5 for treatment groups. **(A, B):** Colorized representative two-dimensional axial microcomputed tomography images. A scale bar below indicates colorization at various thresholds. **(C):** Relative BV. Values are normalized to hSVF + DBX only. Threshold 100 was used. **(D):** Relative BMD. Values are normalized to hSVF + DBX only. **(E, F):** Representative hematoxylin and eosin images at low **(E)** and high **(F)** magnifications. $n = 8$ implants per cell type, $n = 1$ patient specimen. **(G):** Relative lipid droplet number per ×100 field. Means were calculated from 10 random microscopic fields. *, $p < .05$ in comparison with hSVF control; #, $p < .05$ in comparison with hPSC control; **, $p < .05$ in comparison with hSVF with same dose of BMP2. See supplemental online Table 4 for treatment groups. Abbreviations: BMD, bone mineral density; BMP, bone morphogenetic protein; BV, bone volume; cs, cortical shell; eb, ectopic bone; f, femur; hPSC, human perivascular stem cell; hSVF, human stromal vascular fraction.

Figure 5. Effects of NELL-1 on hPSC- or hSVF-mediated ectopic bone formation. hSVF or hPSCs in a SCID mouse muscle pouch with DBX Putty, with or without NELL-1, assessed at 4 weeks postimplantation. See supplemental online Table 6 for treatment groups. **(A):** Representative three-dimensional microcomputed tomography (microCT) reconstructions. Threshold (Th) 90 was used. **(B):** Colorized representative two-dimensional microCT images. A scale bar below indicates colorization at various thresholds. **(C):** Relative BV; Th50−120 used. **(D):** Relative BMD. **(E, F):** Representative hematoxylin and eosin staining at low **(E)** and high **(F)** magnifications. **(G, H):** Histomorphometric analysis of mean bone area **(G)** and mean bone area/tissue area **(H)**, as calculated from 30 random high-powered-fields. $n = 9$ implants per treatment group, $n = 1$ patient specimen. *, $p < .05$ in comparison with hSVF control; #, $p < .05$ in comparison with hPSC control; **, $p < .05$ in comparison with hSVF with same dose NELL-1. See supplemental online Table 5 for treatment groups. Abbreviations: BMD, bone mineral density; BV, bone volume; hPSC, human perivascular stem cell; hSVF, human stromal vascular fraction; NELL-1, Nel-like molecule 1.

Having demonstrated that equal numbers of hPSCs form increased bone as compared with hSVF, we next asked as to whether this difference could be overcome by simply adding more hSVF cells. For this purpose, two concentrations of cells were used in the same intramuscular model: either 2.5×10^4 or 2.5×10^5 cells per implant. All hSVF or hPSC samples were patient-matched. If reduced MSC numbers were the only difference between hSVF and hPSC, then increasing the hSVF cell number 10-fold would surely mitigate any observed differences. However, we found this not to be the case (supplemental online Fig. 1). Namely, hPSCs formed greater bone irrespective of cell
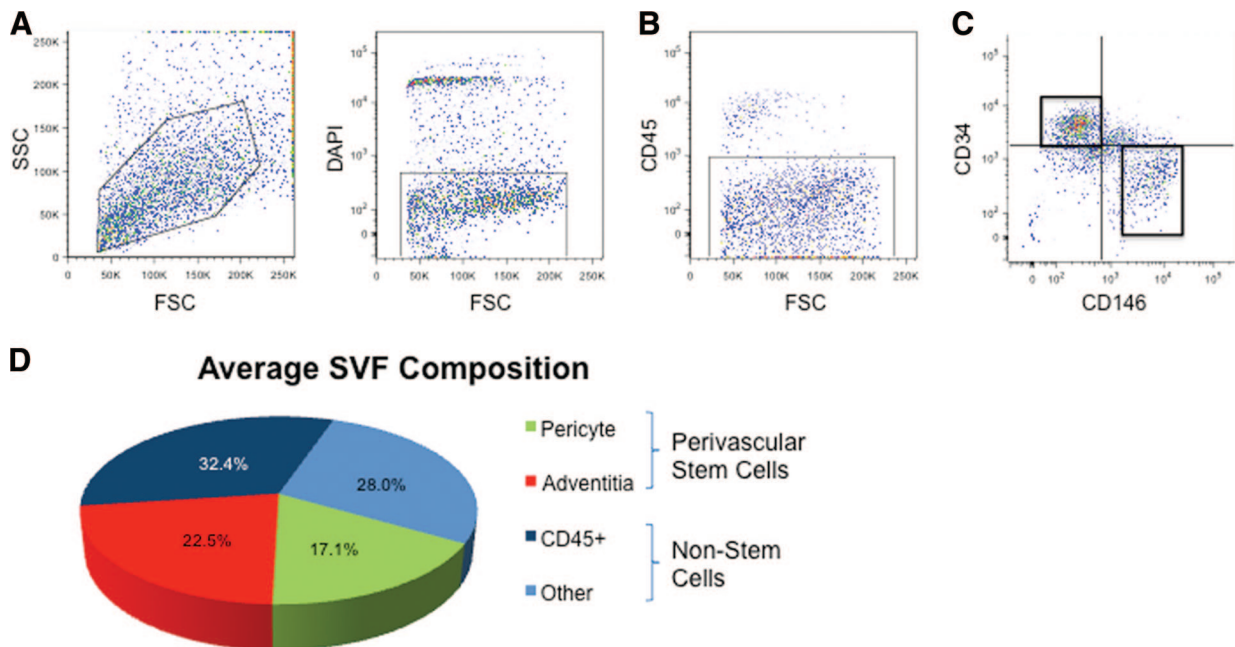
Figure 6. Human white adipose tissue houses distinct pericyte and adventitial cell populations, which together represent perivascular stem cells (PSCs). **(A, B):** After exclusion of DAPI+ dead cells **(A)** and CD45+ hematopoietic cells **(B)**, two PSC populations were isolated with differential expression of CD34 and CD146. **(C):** Distinct CD34+CD146− adventitial cells and CD34−CD146+ pericytes were obtained and combined for in vivo implantation. **(D):** The relative numbers of pericytes and adventitial cells are depicted as a fraction of the total DAPI− SVF cells. Pericytes and adventitial cells make up approximately 17.1% and 22.5%, respectively. PSCs then represent on average 39.6% of total viable cells. Abbreviations: DAPI, 4′,6-diamidino-2-phenylindole; FSC, forward scatter; SSC, side scatter; SVF, stromal vascular fraction.

concentration than hSVF. This was observed by microCT reconstructions of representative samples (supplemental online Fig. 1A), microCT quantifications of BV and BMD (supplemental online Fig. 1B, 1C), and representative histological fields (supplemental online Fig. 1D, 1E). Thus, a simple reduction in stem cell number likely does not explain the difference in bone formation between hSVF and purified hPSC.

BMP2 Promotes hPSC Osteogenic and Adipogenic Differentiation

The most commonly used growth factor for bone regeneration is BMP2 (INFUSE Bone Graft) [35]. We next sought to determine whether BMP2 would be an appropriate stimulus for hPSC bone formation (see supplemental online Table 4 for treatment groups). Two-dimensional axial CT scans showed a clear increase in bone formation among both hSVF- and hPSC-treated samples in response to BMP2 (Fig. 4A, 4B). In addition, a striking trend was observed in which a thin cortical shell (indicated by white arrows in Fig. 4A) was observed in BMP2-treated specimens that extended well beyond the usual ectopic bone margins (Fig. 4A, 4B). Quantification of BV and BMD were next performed with BMP2-treated specimens. First, we again found that BV and BMD were increased in hPSC as compared with hSVF-treated samples (Fig. 4C, 4D, far left). However, the effects of BMP2 were to some extent unexpected. Although BMP2 produced a significant increase in BV (Fig. 4C), it had a negative and opposing effect on BMD as compared with hSVF or hPSC alone (Fig. 4D). Histological evaluation was more revealing (Fig. 4E, 4F). In hSVF and hPSC samples without BMP2, bone chips were closer together (Fig. 4E) and were interspersed with cells with fibroblastic morphology (Fig. 4F, left). In BMP2-treated hSVF or hPSC samples, however, bone chips were farther apart and predominantly interspersed

with lipid droplets (Fig. 4F). In order to quantify the adipogenic response produced by BMP2, relative lipid droplet number per ×100 field was determined. Within both hSVF- and hPSC-treated samples, BMP2 induced a statistically significant increase in lipid droplet number (Fig. 4G). Thus, BMP2 had both pro-osteogenic and also proadipogenic effects within both hSVF- and hPSC-treated implants and may not be the most appropriate cytokine stimulus for induction of hPSC-mediated high-quality bone formation.

NELL-1 Promotes hPSC Osteogenic Differentiation Only

In clinical practice, the only approved growth factor alternative to BMP2 is BMP7 (or OP-1; Stryker, Kalamazoo, MI, http://www.stryker.com); however, BMP7 is also known to have proadipogenic effects [36, 37]. In contrast, NELL-1 is a growth factor in preclinical development that has potent pro-osteogenic effects in small and large mammalian models (reviewed in [38]) and has been recently described to have antiadipogenic effects [26]. NELL-1 was next added to hSVF- or hPSC-laden intramuscular implants (see supplemental online Table 5 for treatment groups). At 4 weeks postimplantation, hPSC-treated implants again showed increased bone formation in comparison with hSVF, as shown by CT reconstructions (Fig. 5A, 5B) and quantification (Fig. 5C, 5D). The addition of NELL-1 led to a significant increase in BV and BMD among hPSC-treated implants (Fig. 5C, 5D, far right column). Histologic and histomorphometric analysis revealed similar findings between treatment groups (Fig. 5E–5H). Bone chips were noted to be closer together among hPSC-treated or hPSC + NELL-1-treated implants (Fig. 5E, 5F). Histomorphometric calculations of bone area and bone area/tissue area confirmed these observations (Fig. 5G, 5H). A significant increase in both parameters was observed between hPSC-treated and hSVF-treated implants. Moreover, hPSC + NELL-1 led

to a significant increase over hPSC treatment alone. Unlike BMP2, minimal lipid was observed among NELL-1-treated samples.

DISCUSSION

Perivascular Cells as a Purified Stem Cell Source

For the first time, we have shown that a purified population of adipose-derived stem cells (hPSCs) is superior to hSVF for bone tissue regeneration. We have shown this in terms of potency (increased bone formation over unsorted hSVF), identity, and purity (defined cell surface markers yielding an MSC population of increased homogeneity without extraneous materials and other cell lineages, such as hematopoietic and endothelial). In theory, hPSCs would also demonstrate improved potency over hSVF, as a defined and homogeneous cell population would have more predictable in vivo outcomes than a nonhomogeneous mixture. Moreover, hPSCs are an attractive cell source, as they are plentiful within adipose tissue (on average constituting ~40% of total viable hSVF). In this regard, even those patients with minimal excess body fat could donate autologous fat tissue for hPSC harvest. Moreover, sufficient quantities of hPSCs could be harvested without the need for time-consuming and costly in vitro expansion. Avoidance of in vitro expansion also reduces the risk of immunogenicity, infection, and genetic instability [12, 13].

Mechanisms of hPSC Improved Osteogenicity

Although hPSCs showed improved bone formation in comparison with hSVF cells across all experiments and all parameters, the underlying mechanism by which hPSCs produce higher bone formation is only partially elucidated. One explanation is that hSVF simply contains fewer MSCs than a purified hPSC population. However, our experiments refute this hypothesis. For example, adding hSVF cells at a 10:1 ratio in comparison with hPSCs still led to inferior bone formation (supplemental online Fig. 1). Another possible explanation is that within hSVF there exists a differentiation-inhibiting cell type. In this regard, endothelial cells have been described to negatively regulate the differentiation of MSCs, such as ASCs or BMSCs [39, 40]. For instance, human endothelial cells inhibit BMSC differentiation into mature osteoblasts by interfering with Osterix expression [40]. With this evidence in mind, hPSCs (which are CD31−) may show enhanced bone formation in part by elimination of the endothelial cell component. Finally, the trophic effect of hPSCs should not be overlooked. Perivascular cells have been observed to secrete high levels of pro-osteogenic, provasculogenic growth factors, such as vascular endothelial growth factor, fibroblast growth factor 2, and epidermal growth factor [24]. PSCs may induce robust in vivo bone formation largely through trophic effects via paracrine induction of vasculogenesis and osteogenesis.

Choice of Osteoinductive Growth Factor

The marriage of an osteocompetent cell source with osteoinductive growth factors is a logical union for skeletal tissue engineering. We examined both BMP2 and NELL-1 as candidate growth factors. BMP2 (INFUSE Bone Graft) is the main FDA-approved osteoinductive factor, but it has significant undesirable side effects, including life-threatening cervical swelling [41], osteoclast activation [42], adipogenic differentiation [43], and bone cyst formation [44, 45]. In particular to our study, we found that BMP2 induced a massive adipogenic response and showed poor

bone quality (reduced bone mineral density) (Fig. 4). This is in line with BMP2's known effects in enhancing the transcription and activity of peroxisome proliferator-activated receptor γ, the main transcription factor regulating adipocyte lineage commitment [46, 47]. In contrast, NELL-1 showed a more osteospecific response, with no apparent induction of adipogenesis (Fig. 5). Our laboratory's previous publications show that exogenous NELL-1 induces significant bone formation in such models as critical sized rat calvarial defects [45]; rat femoral segmental defects [48]; and spinal fusion in rat [30, 49], sheep [50], and nonhuman primate models (manuscript in preparation). The pro-osteogenic effect of NELL-1 was also recently reported using pericytes derived from fetal pancreas in an intramuscular ectopic bone environment [32].

CONCLUSION

In summary, these data show that hPSCs are readily obtainable from human lipoaspirate. Moreover, hPSCs are able to form bone in vivo without the need for predifferentiation. Next, uncultured hPSCs were observed to be superior to patient-matched hSVF with respect to the quantity and quality of bone formation. Finally, through a series of in vivo experiments, we have optimized a combination product for local bone formation by delivering autologous, purified adult hPSCs and an osteoinductive protein (NELL-1) on an acellular allograft bone scaffold.

PSCs not only show improved efficacy in bone formation relative to sample-matched hSVF but also show improvements in other parameters for FDA approval. These include enhanced purity and identity (PSCs are an MSC population containing no hematopoietic stem cells, endothelial cells, or nonviable cells), and potency (as a more defined cell population, hPSCs will likely have reduced variability in effect as compared with hSVF). In fact, the intramuscular implantation assay described may well serve as an easily replicable assay for hPSC potency in bone formation. Excitingly, recent studies have already demonstrated the utility of perivascular stem cells for regeneration of disparate tissue types, including skeletal muscle [51], lung [52], and even myocardium [25]. Further studies will extend our findings and apply the robust osteogenic potential of hPSCs to the healing of bone defects.

AUTHOR CONTRIBUTIONS

A.W.J. and J.N.Z.: conception and design, collection and/or assembly of data, data analysis and interpretation, manuscript writing; X.Z., R.G., and J.S.: collection and/or assembly of data, data analysis and interpretation, manuscript writing; A.A., M. Chiang, W.Y., L.C., M. Corselli, and S.P.: collection and/or assembly of data, data analysis and interpretation; D.S. and B.W.: provision of study material; K.T.: financial support, administrative support, manuscript writing; B.P. and C.S.: conception and design,

financial support, administrative support, manuscript writing, final approval of manuscript.

REFERENCES

1 Zuk PA, Zhu M, Ashjian P et al. Human adipose tissue is a source of multipotent stem cells. Mol Biol Cell 2002;13:4279–4295.

2 Zuk PA. The adipose-derived stem cell: Looking back and looking ahead. Mol Biol Cell 2010;21:1783–1787.

3 Laurencin C, Khan Y. Bone Graft Substitute Materials. emedicine 2004. Available at http://emedicine.medscape.com/article/1230616-overview. Accessed February 16, 2012.

4 Laurie SW, Kaban LB, Mulliken JB et al. Donor-site morbidity after harvesting rib and iliac bone. Plast Reconstr Surg 1984;73:933–938.

5 Frodel JL, Jr., Marentette LJ, Quatela VC et al. Calvarial bone graft harvest. Techniques, considerations, and morbidity. Arch Otolaryngol Head Neck Surg 1993;119:17–23.

6 Meliga E, Strem BM, Duckers HJ et al. Adipose-derived cells. Cell Transplant 2007;16:963–970.

7 De Ugarte DA, Morizono K, Elbarbary A et al. Comparison of multi-lineage cells from human adipose tissue and bone marrow. Cells Tissues Organs 2003;174:101–109.

8 Aust L, Devlin B, Foster SJ et al. Yield of human adipose-derived adult stem cells from liposuction aspirates. Cytotherapy 2004;6:7–14.

9 Levi B, James AW, Nelson ER et al. Human adipose derived stromal cells heal critical size mouse calvarial defects. PLoS One 2010;5:e11177.

10 Levi B, James AW, Nelson ER et al. Human adipose-derived stromal cells stimulate autogenous skeletal repair via paracrine Hedgehog signaling with calvarial osteoblasts. Stem Cells Dev 2011;20:243–257.

11 Cui L, Liu B, Liu G et al. Repair of cranial bone defects with adipose derived stem cells and coral scaffold in a canine model. Biomaterials 2007;28:5477–5486.

12 Gad SC. Pharmaceutical Manufacturing Handbook: Regulations and Quality. Hoboken, NJ: John Wiley and Sons, 2008.

13 Dahl JA, Duggal S, Coulston N et al. Genetic and epigenetic instability of human bone marrow mesenchymal stem cells expanded in autologous serum or fetal bovine serum. Int J Dev Biol 2008;52:1033–1042.

14 Müller AM, Mehrkens A, Schafer DJ et al. Towards an intraoperative engineering of osteogenic and vasculogenic grafts from the stromal vascular fraction of human adipose tissue. Eur Cell Mater 2010;19:127–135.

15 Cheung WK, Working DM, Galuppo LD et al. Osteogenic comparison of expanded and uncultured adipose stromal cells. Cytotherapy 2010;12:554–562.

16 Paredes B, Santana A, Arribas MI et al. Phenotypic differences during the osteogenic differentiation of single cell-derived clones isolated from human lipoaspirates. J Tissue Eng Regen Med 2011;5:589–599.

17 Lanza R. Essentials of Stem Cell Biology. Oxford, U.K.: Elsevier, 2009.

18 Levi B, Wan DC, Glotzbach JP et al. CD105 protein depletion enhances human adipose-derived stromal cell osteogenesis through reduction of transforming growth factor beta1 (TGF-beta1) signaling. J Biol Chem 2011;286:39497–39509.

19 Jiang T, Liu W, Lv X et al. Potent in vitro chondrogenesis of CD105 enriched human adipose-derived stem cells. Biomaterials 2010;31:3564–3571.

20 Crisan M, Yap S, Casteilla L et al. A perivascular origin for mesenchymal stem cells in multiple human organs. Cell Stem Cell 2008;3:301–313.

21 Crisan M, Huard J, Zheng B et al. Purification and culture of human blood vessel-associated progenitor cells. Curr Protoc Stem Cell Biol 2008;Chapter 2:Unit 2B.2.1–2B.2.13.

22 Crisan M, Deasy B, Gavina M et al. Purification and long-term culture of multipotent progenitor cells affiliated with the walls of human blood vessels: Myoendothelial cells and pericytes. Methods Cell Biol 2008;86:295–309.

23 Corselli M, Chen CW, Crisan M et al. Perivascular ancestors of adult multipotent stem cells. Arterioscler Thromb Vasc Biol 2010;30:1104–1109.

24 Chen CW, Montelatici E, Crisan M et al. Perivascular multi-lineage progenitor cells in human organs: Regenerative units, cytokine sources or both? Cytokine Growth Factor Rev 2009;20:429–434.

25 Crisan M, Chen CW, Corselli M et al. Perivascular multipotent progenitor cells in human organs. Ann NY Acad Sci 2009;1176:118–123.

26 Corselli M, Chen CW, Sun B et al. The tunica adventitia of human arteries and veins as a source of mesenchymal stem cells. Stem Cells Dev 2012;21:1299–1308.

27 James AW, Levi B, Nelson ER et al. Deleterious effects of freezing on osteogenic differentiation of human adipose-derived stromal cells in vitro and in vivo. Stem Cells Dev 2011;20:427–439.

28 James AW, Pan A, Chiang M et al. A new function of Nell-1 protein in repressing adipogenic differentiation. Biochem Biophys Res Commun 2011;411:126–131.

29 Tsai CH, Chou MY, Jonas M et al. A composite graft material containing bone particles and collagen in osteoinduction in mouse. J Biomed Mater Res 2002;63:65–70.

30 Li W, Lee M, Whang J et al. Delivery of lyophilized Nell-1 in a rat spinal fusion model. Tissue Eng Part A 2010;16:2861–2870.

31 Boden SD, Kang J, Sandhu H et al. Use of recombinant human bone morphogenetic protein-2 to achieve posterolateral lumbar spine fusion in humans: A prospective, randomized clinical pilot trial: 2002 Volvo Award in clinical studies. Spine (Phila Pa 1976) 2002;27:2662–2673.

32 Zhang X, Peault B, Chen W et al. The Nell-1 growth factor stimulates bone formation by purified human perivascular cells. Tissue Eng Part A 2011;17:2497–2509.

33 Parfitt AM, Drezner MK, Glorieux FH et al. Bone histomorphometry: Standardization of nomenclature, symbols, and units. Report of the ASBMR Histomorphometry Nomenclature Committee. J Bone Miner Res 1987;2:595–610.

34 James AW, Theologis AA, Brugmann SA et al. Estrogen/estrogen receptor alpha signaling in mouse posterofrontal cranial suture fusion. PLoS One 2009;4:e7120.

35 Bueno EM, Glowacki J. Cell-free and cell-based approaches for bone regeneration. Nat Rev Rheumatol 2009;5:685–697.

36 Neumann K, Endres M, Ringe J et al. BMP7 promotes adipogenic but not osteo-/chondrogenic differentiation of adult human bone marrow-derived stem cells in high-density micro-mass culture. J Cell Biochem 2007;102:626–637.

37 Tseng YH, Kokkotou E, Schulz TJ et al. New role of bone morphogenetic protein 7 in brown adipogenesis and energy expenditure. Nature 2008;454:1000–1004.

38 Zhang X, Zara J, Siu RK et al. The role of NELL-1, a growth factor associated with craniosynostosis, in promoting bone regeneration. J Dent Res 2010;89:865–878.

39 Rajashekhar G, Traktuev DO, Roell WC et al. IFATS collection: Adipose stromal cell differentiation is reduced by endothelial cell contact and paracrine communication: Role of canonical Wnt signaling. STEM CELLS 2008;26:2674–2681.

40 Meury T, Verrier S, Alini M. Human endothelial cells inhibit BMSC differentiation into mature osteoblasts in vitro by interfering with osterix expression. J Cell Biochem 2006;98:992–1006.

41 Schultz D. FDA public health notification: Life-threatening complications associated with recombinant human bone morphogenetic protein in cervical spine fusion. Available at http://www.fda.gov/MedicalDevices/Safety/AlertsandNotices/PublicHealthNotifications/ucm062000.htm. Accessed March 9, 2012.

42 Kaneko H, Arakawa T, Mano H et al. Direct stimulation of osteoclastic bone resorption by bone morphogenetic protein (BMP)-2 and expression of BMP receptors in mature osteoclasts. Bone 2000;27:479–486.

43 Moerman EJ, Teng K, Lipschitz DA et al. Aging activates adipogenic and suppresses osteogenic programs in mesenchymal marrow stroma/stem cells: The role of PPAR-gamma2 transcription factor and TGF-beta/BMP signaling pathways. Aging Cell 2004;3:379–389.

44 Jeppsson C, Aspenberg P. BMP-2 can inhibit bone healing. Bone-chamber study in rabbits. Acta Orthop Scand 1996;67:589–592.

45 Aghaloo T, Jiang X, Soo C et al. A study of the role of Nell-1 gene modified goat bone marrow stromal cells in promoting new bone formation. Mol Ther 2007;15:1872–1880.

46 Takada I, Kouzmenko AP, Kato S. Wnt and PPARgamma signaling in osteoblastogenesis and adipogenesis. Nat Rev Rheumatol 2009;5:442–447.

47 Takada I, Suzawa M, Matsumoto K et al. Suppression of PPAR transactivation switches cell fate of bone marrow stem cells from adipocytes into osteoblasts. Ann NY Acad Sci 2007;1116:182–195.

48 Li W, Zara JN, Siu RK et al. Nell-1 enhances bone regeneration in a rat critical-sized femoral segmental defect model. Plast Reconstr Surg 2011;127:580–587.

49 Lu SS, Zhang X, Soo C et al. The osteoinductive properties of Nell-1 in a rat spinal fusion model. Spine J 2007;7:50–60.

50 Siu RK, Lu SS, Li W et al. Nell-1 protein promotes bone formation in a sheep spinal fusion model. Tissue Eng Part A 2011;17:1123–1135.

51 Park TS, Gavina M, Chen CW et al. Placental perivascular cells for human muscle regeneration. Stem Cells Dev 2011;20:451–463.

52 Montemurro T, Andriolo G, Montelatici E et al. Differentiation and migration properties of human foetal umbilical cord perivascular cells: Potential for lung repair. J Cell Mol Med 2011;15:796–808.

See www.StemCellsTM.com for supporting information available online.